Hydrogeology Journal
https://doi.org/10.1007/s10040-020-02191-1

PAPER

Evidence of freshened groundwater below a tropical fringing reef

Benjamin Hagedorn[1] · Matthew W. Becker[1] · Nyssa J. Silbiger[2]

Received: 24 December 2019 / Accepted: 21 May 2020
© Springer-Verlag GmbH Germany, part of Springer Nature 2020

Abstract

Submarine groundwater discharge (SGD) is widely acknowledged as a key driver of environmental change in tropical island coral reefs. Previous work has addressed SGD and groundwater-reef interactions at isolated submarine springs; however, there are still many outstanding questions about the mechanisms and distribution of groundwater discharge to reefs. To understand how groundwater migrates to reefs, a series of offshore ^{222}Rn (radon) and submarine electrical resistivity (ER) surveys were performed on the tropical volcanic island of Mo'orea, French Polynesia. These surveys suggest that fresher water underlies the fringing reef, apparently confined by a <1-m-thick low-permeability layer referred to as a reef flat plate. Reef flat plates have been documented elsewhere in tropical reefs as thin, laterally continuous limestone units that form through the super-saturation of calcium carbonate in the overlying marine waters. In other tropical reefs, the reef flat plate is underlain by a highly permeable karstic limestone formation, but the submarine reef geology on Mo'orea is still uncertain. Numerical modeling of two-dimensional reef transects and SGD quantifications, based on water budget and radon/salinity mass balance, support the confining nature of the reef flat plates and indicate important implications for SGD impacts to tropical reefs. Except where incised by streams or local springs, reef flat plates may route SGD to lagoons or to the reef crest 100s of meters offshore. Because groundwater can transport pollutants, nutrients, and low pH waters, the reef flat plate may play an important role in the spatial patterns of reef ecology and coastal acidification.

Keywords Submarine groundwater discharge · Reef flat plate · Volcanic aquifer · Island hydrology

Introduction

Nearly 200 years after Darwin first puzzled over the abundance of life on tropical islands in an ocean nutrient desert (Darwin's Paradox), researchers are still fitting the pieces together. A growing body of evidence suggests that many biogeophysical drivers shape marine ecological processes surrounding tropical islands, among them, surface and subsurface hydrologic runoff (Gove et al. 2016). In the past decade, new evidence has emerged that submarine groundwater discharge (SGD) carries critical nutrients to reef ecosystems (e.g., Amato et al. 2016; Lubarsky et al. 2018; Prouty et al. 2017; Richardson et al. 2017) and possibly helps buffer reefs against the influence of ocean acidification due to elevated alkalinity in the groundwater (Cyronak et al. 2013); although, some locations show evidence of depleted alkalinity in groundwater which could exacerbate ocean acidification (Richardson et al. 2017). However, most of these studies involved opportunistic sampling in areas surrounding well-mapped submarine springs with visible groundwater discharge. Few studies have taken a holistic look at mechanisms of SGD and the hydrogeology of island reef systems. As a result, site measurements of discharge and their impact on reef ecosystems may not be correctly upscaled to island-wide fluxes.

This paper documents a hydrogeologic investigation of the distribution of SGD to a fringing reef in Mo'orea, a high tropical island in French Polynesia, South Pacific. The purpose was to characterize the mechanism by which groundwater discharges to the reef. Although previous studies on the island have documented evidence of groundwater fluxes to the reef (Haßler et al. 2019; Knee et al. 2016), the contribution of fresh groundwater has not been conclusively separated from recirculated seawater or surface water. This study applies the radioisotope ^{222}Rn (hereafter referred to as radon) to identify and quantify groundwater fluxes to the water column above

✉ Benjamin Hagedorn
Klaus.Hagedorn@csulb.edu

[1] Department of Geological Sciences, California State University, Long Beach, CA 90840, USA

[2] Department of Biology, California State University, Northridge, CA 91330, USA

Published online: 27 June 2020

the reef and electrical resistivity (ER) imaging to identify groundwater below the reef. The study furthermore developed a numerical model that demonstrates the potential for freshened groundwater to underflow the coral reef at significant distances away from the shoreline.

Background

Typically unseen and rarely measured, SGD represents a key pathway for solutes to coral reef ecosystems (Cuet et al. 2011; Cyronak et al. 2014; Garrison et al. 2003; Knee et al. 2010; Nelson et al. 2015; Paerl 1997; Paytan et al. 2006; Peterson et al. 2009; Povinec et al. 2012; Rad et al. 2007; Street et al. 2008; Tait et al. 2013). High volcanic islands generally produce large rates of fresh SGD due to steep seaward hydraulic gradients and aquifers with large hydraulic conductivities (Cuet et al. 2011; Cyronak et al. 2014; Haßler et al. 2019; Knee et al. 2016, 2010; Povinec et al. 2012; Rad et al. 2007; Street et al. 2008; Tait et al. 2014, 2013; Wang et al. 2014). Low carbonate atolls, by contrast, produce less fresh SGD (Cyronak et al. 2014; McMahon and Santos 2017; Santos et al. 2010) as their smaller surface area and shallow topographies induce flatter hydraulic gradients. While there is a general consensus on the detrimental effects of the SGD yield of anthropogenic nutrients (those derived from agriculture and/or septic waste) on reef functioning (Amato et al. 2016; Silbiger et al. 2018), debate is ongoing regarding the impact of SGD solute yield in undisturbed settings. Cyronak et al. (2013) noticed elevated alkalinity from fresh SGD at a fringing reef site at Rarotonga (Cook Islands) and hypothesized that this alkalinity yield could play a key role in counteracting the reef degradation effects of ocean acidification. These findings contrast with results from the Hawaiian Archipelago (Pacific Ocean, USA) or the Yucatan Peninsula in Mexico, where fresh SGD was found to reduce pH and/or alkalinity and to exacerbate the effects of reef degradation (Crook et al. 2012; Prouty et al. 2017; Richardson et al. 2017). While the impact of fresh SGD on biogeochemical cycles in the coastal zone has been widely acknowledged, recent research pointed out the challenge of understanding the spatial and temporal dynamics of SGD in light of hydrogeological heterogeneities in coastal aquifers and seasonality in recharge (Montiel et al. 2018). Previous studies addressed SGD rates and coral reef ecosystem response primarily at opportunistic locations; i.e. at "bubbling" spring sites identified from anecdotal evidence. The failure to correctly account for hydrogeologic heterogeneity in the terrestrial/reef coupling has likely led to the conflicting assessments of solute fluxes to island reefs. A comprehensive analysis of how SGD is delivered to coral island reefs is lacking.

Groundwater flow on high volcanic islands such as Hawai'i, Tahiti (French Polynesia), Montserrat in the Caribbean Sea (UK), etc. occurs principally in lava flows and associated sediments characterized by high conductivity and storage capacity (Hemmings et al. 2015; Hildenbrand et al. 2005; Lau and Mink 2006; Oki et al. 1998; Rougerie et al. 2004). Towards the coastal plains, these volcanic aquifers are often covered by a sedimentary wedge (Fig. 1) composed primarily of alluvial sediments as well as paleo-reef deposits and organic debris of the eroded volcanic flanks (Oki et al. 1998). On Hawai'i, these sediments can form a confining unit and inhibit the free discharge of fresh groundwater to the reef, raising hydraulic heads in the layered basalt aquifers below (Gingerich and Voss 2005; Rotzoll et al. 2010).

Groundwater flow to a fringing island reef is often represented by a simple dual aquifer model (Bailey et al. 2010, 2009; Werner et al. 2017). These aquifers are associated with lower-permeability Holocene deposits above and high-permeability Pleistocene deposits below, separated by the 15–25 m deep "Thurber Discontinuity" (Vacher 2007; Fig. 1). This stratigraphic unconformity results from eustatic sea level changes that eroded the Pleistocene reef to a platform that formed the basis of the younger post-glacial reef (Dickinson 2004). Diagenesis during the Pleistocene typically results from karstification of the Pleistocene formations, leading to hydraulic conductivities that are orders-of-magnitude greater than the Holocene deposits above (Bailey et al. 2009; Falkland 1994). The larger hydraulic conductivity in the Pleistocene strata results in an effective truncation of the freshwater lens at the Thurber Discontinuity (Werner et al. 2017) due to seawater mixing.

A key hydrogeologic feature of many coral atolls is the reef flat plate, which is a shallow (1–1.5 m depth) impermeable apron of well-cemented reef rock that underlies the reef and that acts as a confining unit for submarine aquifers (Anthony 2004; Ayers and Vacher 1986; Bailey et al. 2008; Oberdorfer and Buddemeier 1986; Rougerie et al. 2004; Werner et al. 2017; Figs. 1 and 2). Ayers and Vacher (1986) reported a two or three order-of-magnitude difference in hydraulic conductivity between the reef flat plate and underlying sediment facies on Deke Island Atoll, Micronesia. The extent of the reef flat plate varies, but on Deke, it extends from about the midpoint of the island to offshore below the fringing reef. The authors stated that because of the confining presence of the reef flat plate, on Deke Island "*…it is not appropriate to assume that the ocean shoreline of the island marks a discharge boundary. In fact, groundwater must be transported well beyond the island limits to exit either through the reef flat or, probably in some cases, along the reef margin itself.*"

The diagenesis of reef flat plates has not yet been investigated. Submarine lithification is well documented and is considered to be common in modern tropical reefs (Macintyre 2011, 1977). Studies suggest that submarine lithification occurs primarily near the sediment/seawater interface due to supersaturation of carbonate in tropical sea water (Parnell 1986). Rougerie et al. (2004) note that this lithification can reduce

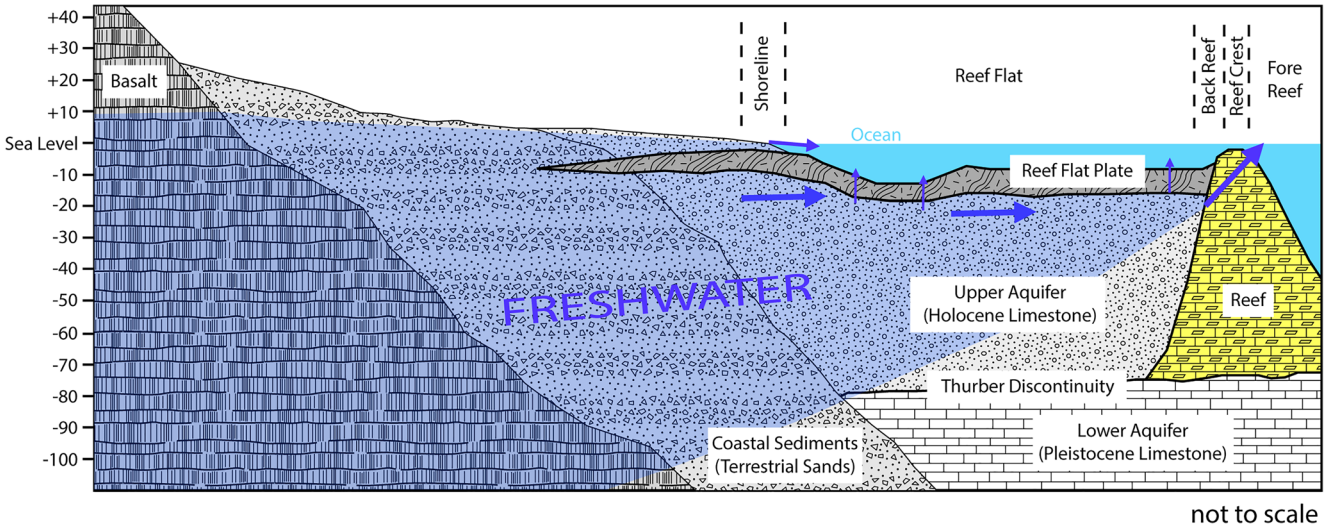

Fig. 1 Conceptual framework of fresh SGD (blue arrows scaled for magnitude) at a volcanic island barrier reef. Modified after Ayers and Vacher (1986) and Gingerich and Voss (2005)

flow between the water column and the subreef. MacIntyre (1977) describes highly lithified limestone agglomerate in which the aragonitic reef structure has been almost completely replaced by magnesium carbonate, cemented debris, and noncarbonate grains in the modern reef off Galeta Point, Panama. However, to the authors' knowledge, the controls on the morphology of the reef flat plate have not been fully explored. Although Ayres and Vacher (1986) describe in great detail how the reef flat plate of Deke Island is thickest at the live reef barrier and pinches out about mid island, they do not suggest a mechanism for this structure. It may be that water exchange is greater near the edge of the reef due to tidal and wave pressures (Tribble et al. 1992), which promotes cementation and a thicker reef plate. Thinning closer to the coast and below terrestrial sediments could also be due to the introduction of lower-pH meteoric water, but support of this hypothesis was not found in the literature.

Compared to coral atolls, very little is known about the role of the reef plate for the hydrodynamics of groundwater on volcanic islands. Several studies (Grossman et al. 2006; Rougerie et al. 2004) reported the presence of a continuous low porosity/permeability layer, e.g., the "pavement facies" described by Grossman et al. (2006), within just a few meters of the seafloor of fringing reefs in Hawai'i. On Mo'orea, reef plates are well known to the local community because of their resistance to excavation

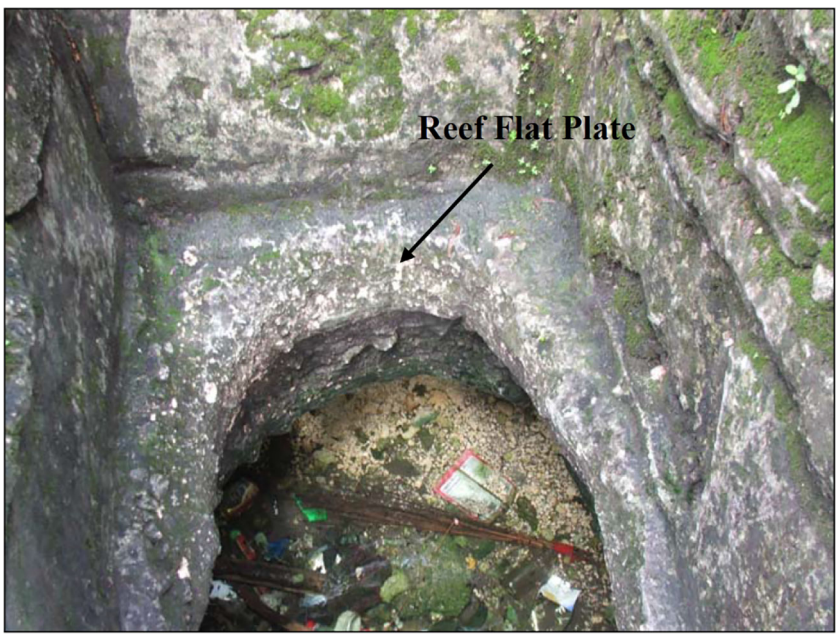

Fig. 2. Example of well-cemented reef plate unit, exposed in a well on Mogmog Island, Ulithi Atoll of Micronesia (reproduced from Bailey et al. 2008)

in the process of construction. Similar features have been documented on atolls (see Fig. 2).

Hydraulic modeling on atolls and volcanic islands tend to focus on freshwater resources, i.e., the freshwater lens (Gingerich and Voss 2005), and consequently are not of sufficiently fine resolution to resolve coastal discharge in general and reef flat plates, in particular. Houben et al. (2018) used physical and numerical modeling to show that impermeable units similar to the reef flat plate underneath fringing reefs lead to a bimodal distribution of fresh SGD. The authors noticed only minor "diffuse" SGD at the beach face and significantly higher rates of "underflow" SGD around the rim of the confining unit; potentially at significant distances from the coast. Even though the role of the reef flat plate has not been specifically addressed in previous SGD assessments, it may very well explain the uneven distribution of fresh SGD that was traced via nearshore surveys of radon on the Island of Rarotonga (Cook Islands; Tait et al. 2013) and along the Mexican Yucatan Peninsula (Null et al. 2014; Parra et al. 2015). Other pathways of reef underflow have been identified and may occur in conjunction with reef plate confinement. Null et al. (2014), for example, stressed the importance of submarine karst features generated by CO_2-rich groundwater as conduits for fresh SGD to occur at isolated submarine springs (or "ojos"). Cardenas et al. (2010) highlighted the role of faults to generate fresh SGD springs across a reef off a low carbonate island of the Philippines. For volcanic islands, several studies have shown the importance of submarine volcanic features such as lava tubes as conduits for fresh SGD (Dimova et al. 2012; Garrison et al. 2003; Tait et al. 2013). Although these features can generate extremely large flows of fresh SGD, they tend to be highly localized.

Coastal stream channels are particularly important for SGD in volcanic island settings. Streams can incise reef flat plates at the coast, which may breach hydraulic confinement and potentially create a localized enhancement of fresh SGD from (1) diffuse seepage from the beach face and (2) trapped SGD that originates from lateral flow beneath the reef plate. Through these processes, stream channels could yield year-round pulses of fresh SGD that deliver nutrients and potentially pollutants to the live reef. However, it is difficult to specifically separate stream discharge from groundwater underflow (i.e., SGD) as they tend to display overlapping geochemical (i.e., salinity) signatures, thus complicating upscaling to island-wide SGD estimation.

Although every tropical island and its reef system is unique, the literature indicates a surprising commonality with respect to the reef structure and apparent hydrogeology. All tropical fringing reefs appear to at least have the potential to form reef plates and these reef plates have the potential to isolate freshwater SGD from the reef. Recent studies predict that an acidifying ocean will begin to dissolve many tropical reefs in the coming decades (Eyre et al. 2018, 2014). A change in the chemical equilibrium may cause these plates to degrade, which would ultimately release more freshwater to the reef. The elevated nutrients and low pH waters from an increased groundwater flux could disrupt reef ecosystem functioning and compound the negative effects of ocean acidification on coral reefs (Silbiger et al. 2018).

The guiding hypothesis of this study is that reef flat plates can be a similarly important hydrogeologic feature on reefs surrounding high volcanic islands as they are on low elevation atolls. To test this hypothesis, radon surveys, geographic information system (GIS)-based water budgets and ER profiles were used to (1) quantify SGD at distinct transect sites and (2) document the presence of confined freshwater below the reef, that might indicate the presence of a confining layer consistent with a reef flat plate. Finally, numerical models were developed to elucidate how freshwater buoyancy might be expressed in such a confining layer below the reef flat.

Materials and methods

Local setting: Mo'orea

This study was carried out on the tropical island of Mo'orea, French Polynesia, located about 20 km west of Tahiti (Fig. 3). The island is of historical significance as Darwin solidified his theory of reef evolution from fringing, to barrier, to atoll, while observing Mo'orea from a high-point on Tahiti. Mo'orea is a high-elevation (<1,207 m above sea level) volcanic island with a barrier reef subject to large fresh groundwater inputs (Hildenbrand et al. 2005; Rougerie et al. 2004). Reef-pass channels occur on Mo'orea approximately every 5–10 km around the circumference of the island. Climate is typically tropical humid with warm year-round temperatures (~25°C) and a pronounced wet season from November to March. Data were collected in early January of 2019, but the wet season had not yet begun in earnest. Ephemeral streams were not flowing and rain was intense, but of short duration during and prior to data collection.

Mo'orea is the home of Mo'orea Coral Reef Long Term Ecological Research (MCR LTER) site and is one of the most investigated reef systems of the Pacific (Edmunds et al. 2018). Only a few SGD studies have been conducted on Mo'orea to date. Knee et al. (2016) compiled shore-perpendicular surface-water transects of the groundwater tracers ^{223}Ra, ^{224}Ra, ^{228}Ra and salinity at Paopao Bay, the largest coastal embayment and outlet of one of the island's few perennial streams. They noticed relatively low fresh SGD components in Paopao Bay which they determined from high $^{223, 224, 228}$Ra isotope activities co-occurring with seawater salinities. Low fresh SGD was attributed to sampling taking place in the dry season. Haβler et al. (2019) did not quantify SGD rates on Mo'orea, but investigated sources of nutrients in coastal waters and

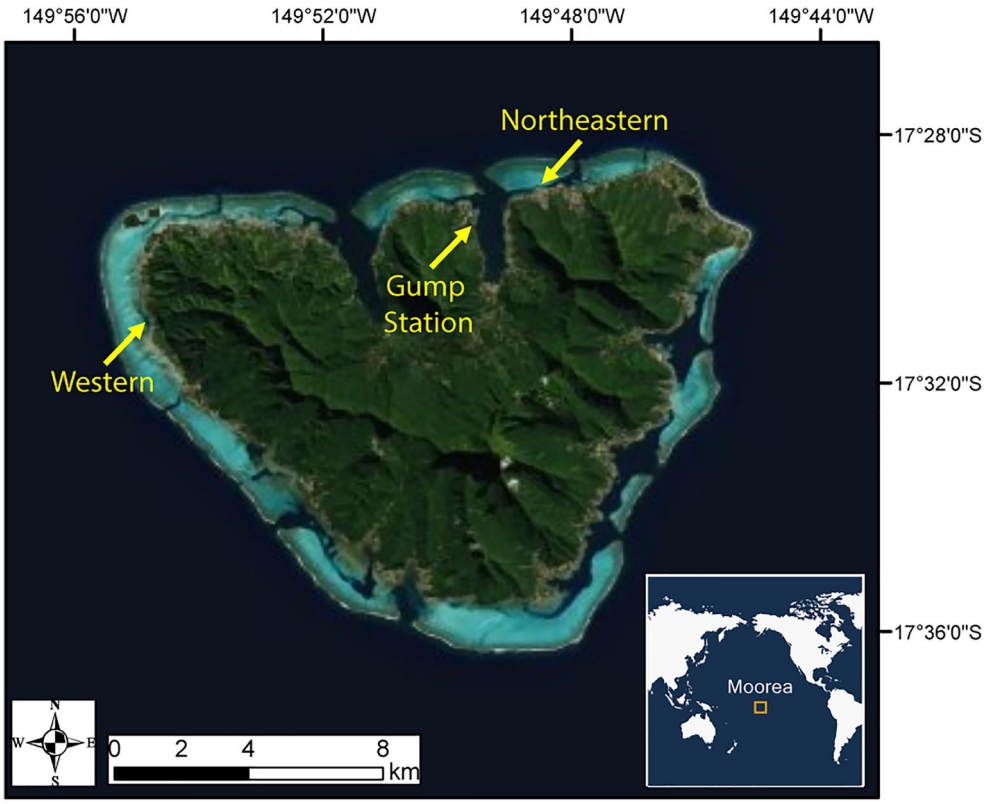

Fig. 3. Location of the study area, the island of Mo'orea in French Polynesia, Pacific Ocean. Arrows depict the Northeastern, Gump Station, and Western study sites. Index map reproduced from Dubé et al. (2017).

found that nutrient yields from fertilizer and septic waste/manure applications were very low.

Three sites in which both radon sampling and electrical resistivity profiling were conducted are presented herein (Fig. 3). These sites are referred to as the *Northeastern*, *Western*, and *Gump Station* transects. The latter is named for the Richard B Gump University of California Berkeley Field station from which these study activities were based. All data were collected on the near shore fringing reef at <5m depth.

Submarine groundwater discharge analysis

Radon surveying

Radon has shown to be a useful tracer for SGD analysis (Burnett et al. 2006; Burnett and Dulaiova 2003) because of its inert nature and the fact that it attains a distinct groundwater signature very shortly after infiltration, i.e., when it reaches secular equilibrium with parent nuclide ^{226}Ra, which is only about 28 days (Cecil and Green 2000). Given this, groundwater radon variability is more impacted by factors related to groundwater emanation such as aquifer mineralogy, and texture (i.e., grain shape and size) rather than seasonality in recharge (Barillon et al. 2005; Cook et al. 2003). Moreover, radon tends to be significantly depleted in surface water because of its volatility and short radioactive half-life (about 3.8 days).

Spatial radon surveys were conducted at the Northeastern and Western transects with a kayak moving at <5 km/h. Time series data were collected at the Northeastern and Gump Station sites. Water was collected at about 30 cm below the water surface via a battery-powered 1100 GPH Rule bilge pump attached to a Durridge RAD AQUA air-water exchanger. The air from this exchanger was run through a desiccant drying unit before entering a Durridge RAD7 radon analyzer. The RAD7 counts the positively charged polonium daughter ^{218}Po as a measure of the radon concentrations and then converts those to concentrations in water as a function of the radon transfer coefficient at the given water salinity and temperature. The radon counts for spatial surveys were averaged over 6-min cycles, while time-series data were averaged over 30-min cycles. Importantly, radon-in-water concentrations that are detected via radon in-air detectors (such as the RAD7) demonstrate a distinct response delay between radon-in-water and related radon-in-air records due to the kinetics of the related water/air phase transition and the ^{218}Po decay constant (Petermann and Schubert 2015). As a conservative approach to account for this delay (Schubert et al. 2019), raw radon data was shifted backwards by 24 min.

No groundwater wells were accessible for this study, but coastal spring water was sampled about 300 m east of the Western transect shoreline. Spring water was collected from an about 50 cm deep excavation via a battery-powered 1100 GPH Rule bilge pump attached to the Durridge RAD AQUA

air-water exchanger and the Durridge RAD7 radon analyzer. The pump was run for approximately 100 min prior to radon analysis to ensure sampling of non-degassed formation water and radon counts were averaged over 10-min cycles.

Conductivity, temperature, and depth (CTD) were monitored using HOBO U24-002-C and InSitu Aqua Troll 600 probes at the pump hose inlet at 1-min intervals. Wind speed data for atmospheric radon loss computations were collected at Gump Station and at Hotel Les Tipaniers, about 2.5 km north of the Western transect.

Radon-based SGD quantification

Radon measurements from the surveys were converted into SGD fluxes F_{SGD} (dpm/m^2/day) following Schubert et al. (2019) by subtracting radon sources, specifically radioactive production within the water column (F_{prod}), from the sinks; i.e., are radon decay (F_{dec}), offshore shore radon mixing loss (F_{mix}) and atmospheric radon degassing (F_{atm}):

$$F_{SGD} = F_{mix} + F_{dec} + F_{atm} - F_{diff} - F_{prod} \quad (1)$$

This approach assumes negligible radon input from surface water and pore water diffusion from marine sediments (Oehler et al. 2019a; Tait et al. 2013). Based on the radon concentration of the SGD groundwater end-member (dpm/m^3), F_{SGD} and the related radon flux was converted into the actual SGD water flux (m/day).

Because spatial survey measurements only present snapshots of a tidal cycle, all radon data were tide-corrected. Ideally, this correction can be done through a simple regression analysis of radon and tide time series (Schubert et al. 2019). On Mo'orea, however, there was no statistically significant ($p < 0.05$) correlation between these parameters; an observation that agrees with those from other tropical island settings with reduced freshwater SGD (Bishop et al. 2017; Cyronak et al. 2014). Given this, data were tide-corrected by projecting the mean measured radon inventory, I (dpm/m^2), defined as the product of the measured radon value and water depth, to a tidal mean inventory deduced from concurrently measured radon and tidal stage time series; the latter sourced for Papeete station from the University of Hawai'i, Sea Level Center. Technical issues prohibited collection of time series data for a full tidal cycle assessment at the Northeastern transect. As a simplified solution, this study applied the available 4-h average value (Fig. 4b) as a proxy; noting that this should be considered a lower limit of SGD as the time frame coincided with the rising limb of the diurnal cycle (Fig. 4b). Likewise, at the Western transect, technical malfunctions prevented the collection of any time series data. In this case, no tidal correction was applied, but, because sampling took place right within the mid-point between low and high tides, results are considered cursory estimates of tidally scaled SGD.

Quantification of radon fluxes F_{prod} and F_{dec} in coastal water are defined by the concentration ^{226}Ra (~79.8 dpm/m^3; (Bojanowski 1988)) and the radon decay constant (0.181 day^{-1}), respectively. F_{mix} can be constrained as a function of the radon inventory I and water residence time τ (days) assuming that the mixing intensity between offshore and coastal water increases as an exponential function with the distance to the shoreline (Schubert et al. 2019):

$$F_{mix} = I \times \left(1 - e^{-\frac{1}{\tau}}\right) \quad (2)$$

In many previous studies, τ has been linked to tidal frequencies, but in a microtidal setting like Mo'orea where the tidal amplitude is <30 cm, water mixing has shown to be more controlled by wave-driven circulation and, to a lesser degree, wind-driven currents (Hench et al. 2008; Leichter et al. 2013). To account for these nontidal mixing controls, site-specific water residence time can be calculated from ^{224}Ra/^{223}Ra activity ratios (ARs) of coastal water and groundwater samples. No ^{224}Ra/^{223}Ra AR data were available for the present study, but Knee et al. (2016) reported AR data for the Gump Station and Northeastern sites for the austral winter months of 2008. However, no statistically significant differences in AR were observed between groundwater and coastal water sample groups, so specific residence times could not be calculated. It was therefore decided to estimate τ based on reported back reef current data in the literature. Several studies have reported water flow speeds in Mo'orea's back reefs to be fairly consistent around the island and to generally vary between 0.05 and 0.1 m/s (Comeau et al. 2014; Hench et al. 2008; Leichter et al. 2013; Rosman and Hench 2011). Based on the studies by Hench et al. (2008), who defined a water budget for Paopao Bay (near the Gump Station and Northeastern transect sites) of water entering the lagoon over the reef crest and water exiting the lagoon through the reef pass, τ was approximated using data on (1) reef crest fluxes, (2) reef crest water depths and (3) reef crest width (i.e., reef capture zone). These data were reported for the austral summer months of 2004–2005; a time frame similar to that of this study. The resulting τ range of 1.28–7.35 h is lower than the typical semidiurnal tidal cycle (~12 h), thus highlighting the importance of site-specific τ assessments. Following the approach of Kelly et al. (2019), this τ range was used as a measure for F_{mix} uncertainty in this in the F_{SGD} quantification.

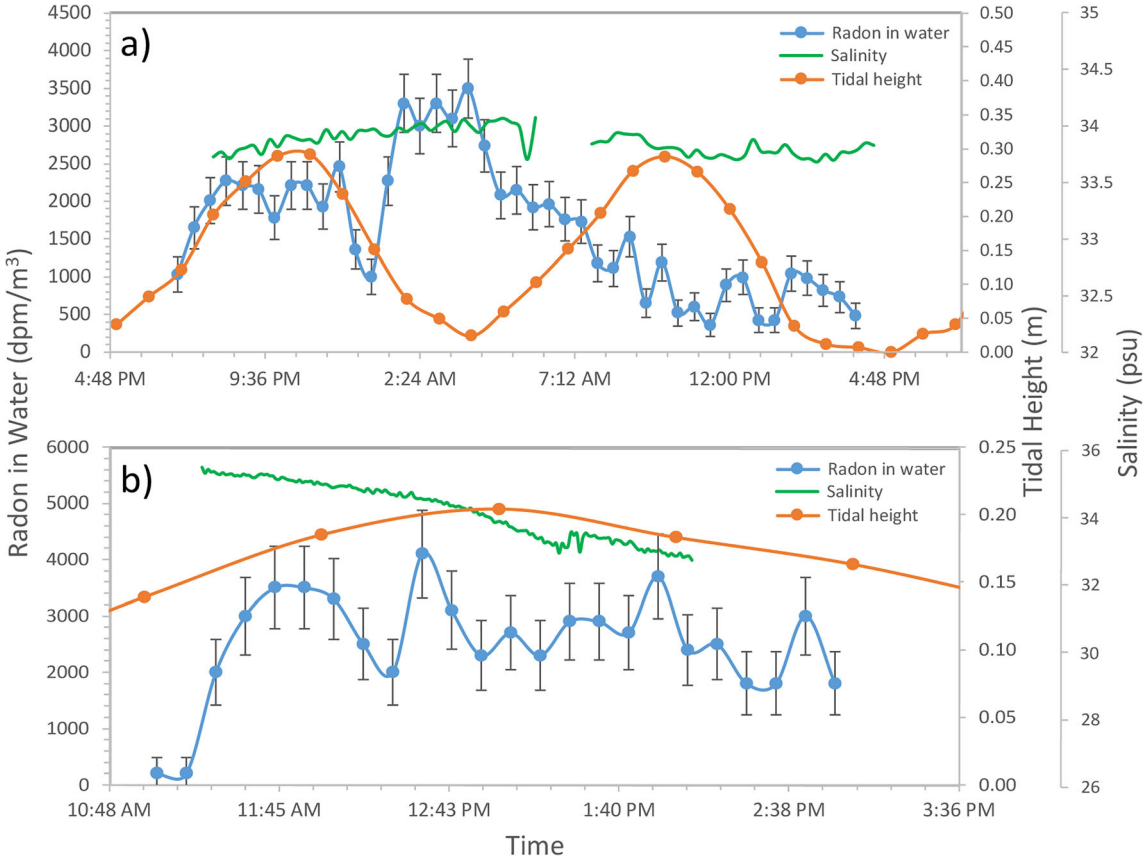

Fig. 4 Time series plot of radon activity, salinity, and tidal stage measured at **a** Gump Station and **b** Northeastern site. Horizontal scale varies from plot to plot in order to optimally display the full range of data

F_{atm} (Fig. 6) was calculated as a function of the wind speed recorded during and up to 4 days prior to the sampling as (Schubert et al. 2019):

$$w_t = e^{[-(\lambda_{radon}+\tau)\times t]} \quad (3)$$

$$F_{atm} = \frac{\sum_{t=0}^{t_{max}}[w(t) \times F_{atm}(t)]}{\sum_{t=0}^{t_{max}} w(t)} \quad (4)$$

where w_t is the weighting factor that quantifies the influence of the previous degassing event for the time step t (day) and λ_{radon} is the radon decay constant (0.181 day^{-1}). $F_{atm}(t)$ is the degassing loss at time step t that was modeled using gas transfer equations presented by Wanninkhof (2014 and references therein) and measurements of temperature, wind speed, atmospheric radon measurements collected in the field (~30 dpm/m^3) and the Ostwald solubility coefficient determined after Weigel (1978). Importantly, water conditions were very calm throughout the surveys. Wind speed varied from 0.2 to 7.0 m/s during the surveys and there was no significant wave action (i.e., whitecaps) at any time of the study.

Conversion to saline and fresh SGD fluxes No wells were accessible during the time of study, so the groundwater radon end-member ($Radon_{GW}$) was set to 116 ± 9 dpm/L based on measured radon activities of a freshwater spring sampled 300 m inland from the Western transect (Fig. 5b). This spring was located in a dried-up stream channel where fluvial sands are juxtaposed with basaltic bedrock. The measured radon value aligns at the lower end of the spectrum observed for groundwater on other volcanic islands (e.g., 25–6,879 dpm/L for Rarotonga Island; Tait et al. 2013). Previous research, however, has highlighted groundwater radon values on volcanic islands to be highly variable, particularly towards the coastal plains where reduced radon contributions from carbonaceous beach sediments can "dilute" the groundwater radon signal. However, beach sand pore waters can also exhibit reduced radon (and elevated salinities) if sampled too close to the freshwater/seawater interface. It becomes clear that not capturing the potential groundwater radon variability in the SGD assessments is certainly a limitation of the present study and should be investigated in future research.

For subsequent comparisons, each survey line F_{SGD} value was normalized over watershed surface area and length of the shoreline perimeter. Furthermore, the freshwater fraction of

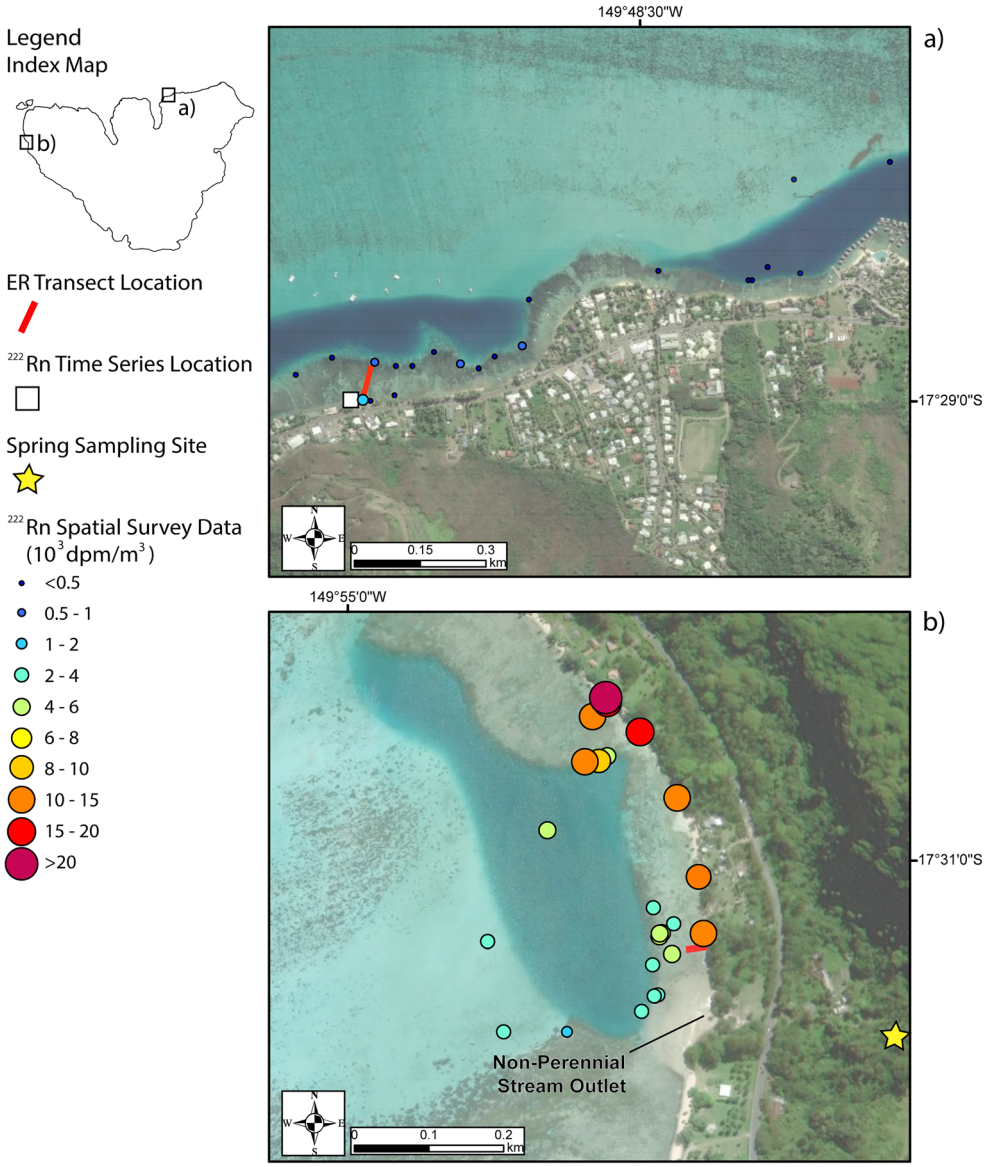

Fig. 5 Spatial radon survey data at the **a** Northeastern and **b** Western sites. Locations of electrical resistivity (ER) profiles and radon time series measurements are shown. Location of Gump Station transect is not shown

F_{SGD} was calculated using a two endmember mixing analysis, as explained by Bishop et al. (2017), with a groundwater (i.e., measured spring water) salinity end-member of 116 mg/L, an ocean water salinity end-member of 35,500 mg/L and the mean salinities of the respective transect samples.

Water budget-based SGD quantification

Water budgets can be used to derive estimates of groundwater recharge (and submarine groundwater discharge) if input parameters on precipitation, fog drip, irrigation, evapotranspiration, surface runoff and changes in groundwater storage are independently constrained (Engott et al. 2017; Harlow and Hagedorn 2019; Izuka et al. 2005; Johnson et al. 2018; Mair et al. 2019). Water that infiltrates below the root zone of the soil-plant system is usually referred to as potential recharge to distinguish it from water that reaches the actual water table in the saturated zone (Hagedorn et al. 2011; Rushton and Ward 1979). The distinction between potential and actual recharge becomes important when the unsaturated zone is thick because the time of travel to reach volcanic aquifers on oceanic islands can be on the order of years or decades (Koh et al. 2006). Nevertheless, in scenarios where long-term input parameter data are available and where groundwater extraction is well defined, estimates of potential recharge from a water budget can serve as a proxy for potential SGD (Sawyer et al. 2016).

Mo'orea, like many other remote oceanic islands, lacks the high resolution (i.e., daily time scale) precipitation and climate data needed for a refined water budget. This is a particular problem as it relates to surface runoff because, on tropical islands, surface runoff can represent up to 30% of the annual

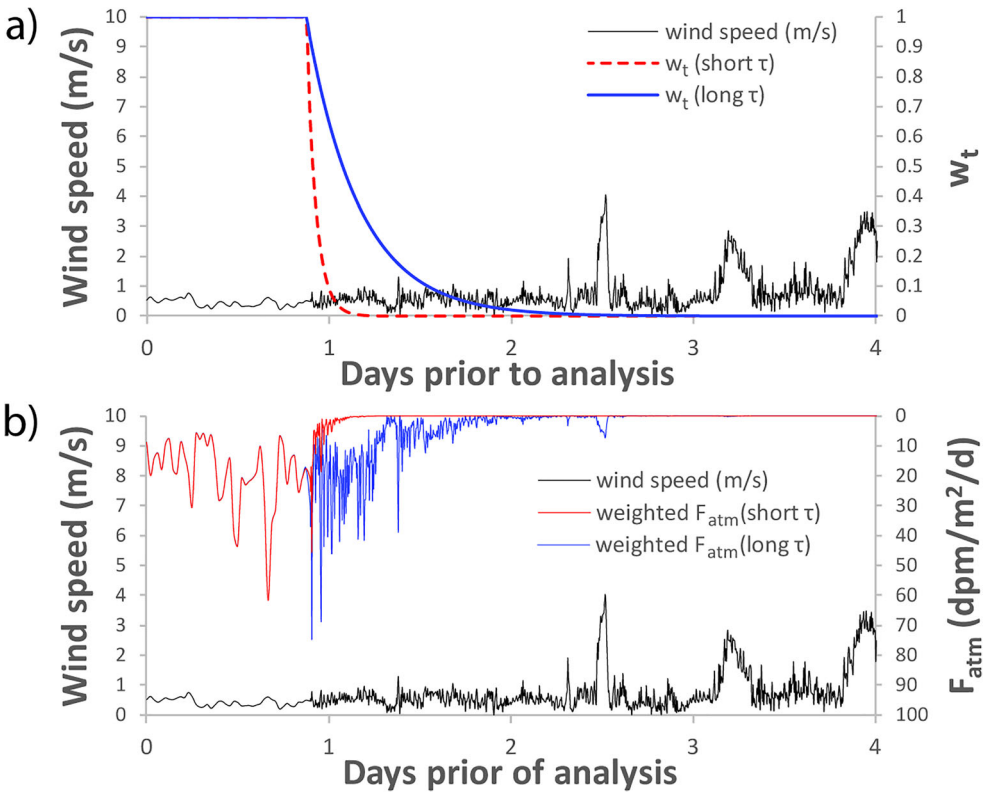

Fig. 6 **a** Weighting functions (w_t) and **b** quantification of weighted atmospheric radon flux (F_{atm}), for two water residence time (τ) scenarios during and prior to the time series sampling at Gump Station. Note the change in temporal resolution from 30 min during radon sampling to 5 min in the days prior to the sampling

mean rainfall input (Izuka et al. 2005; Johnson et al. 2018; Mair et al. 2019) and tends to by highly variable (i.e., "flashy"; Hagedorn et al. 2016; Tomlinson and De Carlo 2003). However, there are currently no publicly available runoff data so direct runoff could not be reasonably estimated. In light of these limitations, and because none of the streams in the sampled watersheds were flowing at the time of study, the approach of Oehler et al. (2019a) was followed and maximum recharge (R) was computed as a proxy for maximum potential SGD for the time of sampling (i.e., January) through a simplified water budget as:

$$R = P - \mathrm{ET} \quad (5)$$

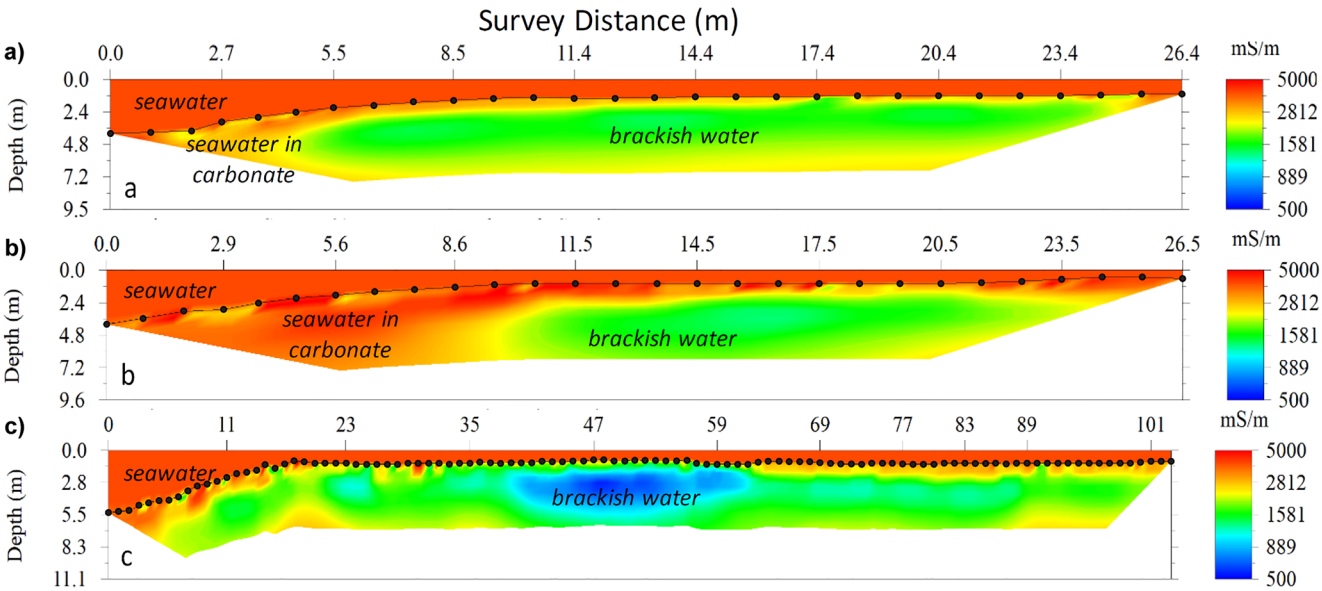

Fig. 7 ER sections acquired from **a** Gump Station, **b** Western, and **c** Northeastern transects. Transects extend from the shoreline (right) into the ocean (left). The location of ER sensors on the seafloor bottom is shown as black circles

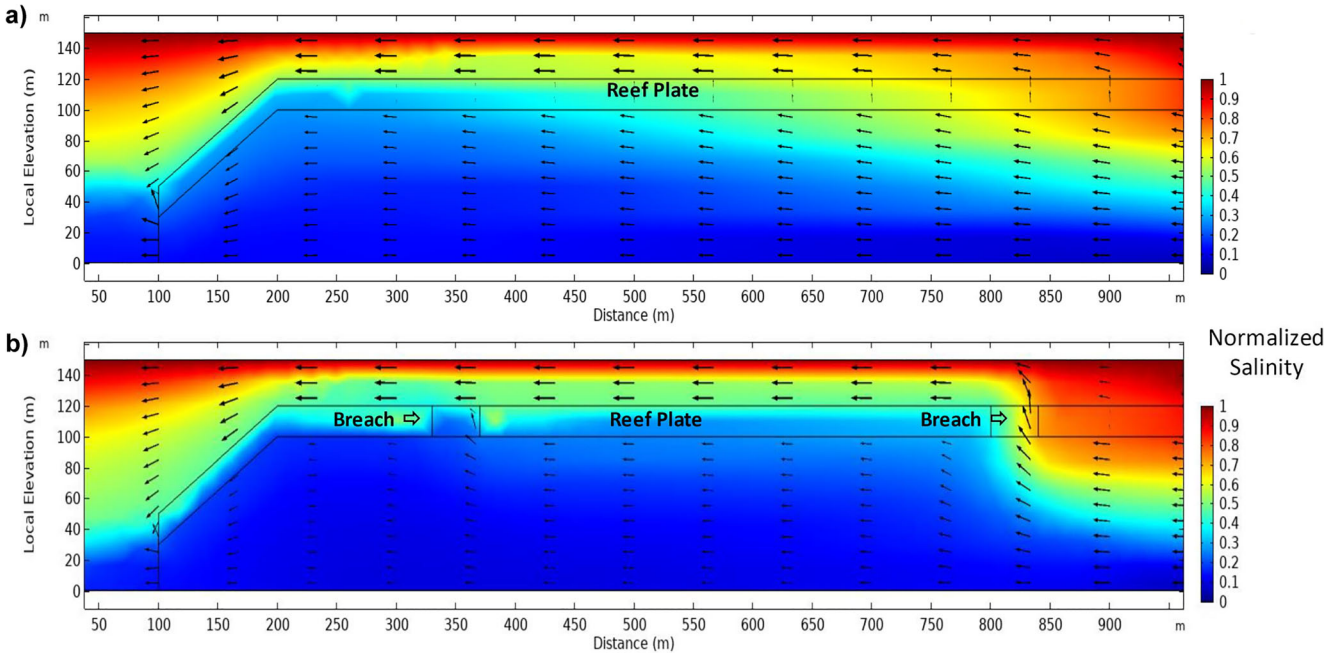

Fig. 8 Numerical simulations of variable-density flow through a reef flat. The reef plate is represented by the black outline. Color is salinity normalized to seawater (35 ppt NaCl); blue is fresh and red is seawater. Arrows are specific discharge vectors. Model scenarios are **a** continuous reef plate and **b** reef plate with a small breaches

where P and ET correspond to mean monthly precipitation and evapotranspiration data, respectively, obtained from global scale WorldClim (Fick and Hijmans 2017; Hijmans et al. 2005) and MODIS (Mu et al. 2011, 2007) databases. A volumetric maximum recharge was estimated by multiplying R with the size of the watershed. That value was then converted to maximum potential SGD (F_{SGDmax}; dpm/m^2/day) by dividing with the length of the watershed shoreline (Table 1).

Electrical resistivity tomography

Electrical resistivity (ER) profiling is a geophysical technique that employs measures of voltage loss between electrodes at the surface, to measure the electrical resistivity of subsurface materials. Converting the surface measurements of ER to an ER profile requires inversion of a model cross-section. Consequently, the profile derived from ER measurements is somewhat nonunique. However, repeating ER measurements, overlap among ER measurements, and swapping polarity of the electrodes can help in identifying poor measurement points and estimate the accuracy of the inversion. This study used EarthImager 2D (AGI, Austin, Texas), which was developed for the resistivity instrumentation used here (Supersting R8, AGI, Austin Texas). The depth of the water column was measured at every electrode such that the topography of the seabed and the thickness of the water column could be properly represented in the model. Because seawater is so highly conductive, the water column leads to current channeling which affects the inversion. For all results presented here, the estimate root mean square (RMS) error was less than 6%, indicating generally robust inversion of the bulk (apparent) electrical resistance profile.

The inverted bulk electrical resistance of the subsurface (ρ_b) is related to the electrical resistance of the pore fluid (ρ_f) through Archie's Law:

$$\rho_b = \rho_f n^{-m} \tag{6}$$

Table 1 Water budget estimates of recharge (R) and associated maximum freshwater SGD (F_{SGDmax})

Study site	Watershed area (m^2)	Shoreline length (m)	Mean P (m/day)	Mean ET (m/day)	Mean R (m/day)	F_{SGDmax} (m^3/m/day)
Northeastern	203 × 10^6	1,351	0.083	0.043	0.039	59.3
Western	1.45 × 0^6	608	0.077	0.042	0.035	84.4
Gump Station	NC	NC	NC	NC	NC	NC

NC not calculated

where n is the connected porosity of the formation and m is an exponent that accounts for the tortuosity of pore connections. Thus, the fluid resistivity, which is linearly related to salinity and the parameter of interest here, is not simply related to the bulk resistivity measured by ER. Decoupling porosity and fluid salinity, consequently, requires information regarding the carbonate reef sediments/rock that were imaged. For unconsolidated sands, m is usually considered to be 2. However, in vuggy carbonates, m may range between 2 and 5, depending on the structure of the pore space (Jackson et al. 2002, 1993). An unfortunate limitation of this study is that the porosity and its tortuosity were not measured, for example, through coring. This limitation has also been noted in other ER measurements in reefs (e.g., Befus et al. 2014).

Electrical resistivity surveys have been one of the most commonly used tools to document submarine groundwater discharge, particularly in reef environments. Most notably, Cardenas et al. (2010) and Befus et al. (2014) have used ER to map subreef freshwater in the fringing reefs of Santiago Island (the Philippines) and Rarotonga (Cook Islands), respectively. These studies showed the ubiquity of freshwater beneath reefs, but were focused on the influence of subsurface geologic features such as lava flows and lineaments rather than the reef structure itself. Most ER studies are conducted using a boat-towed array of ER electrodes, which provides rapid data acquisition with good depth penetration, but sacrifices vertical resolution. In reef environments, towed surveys are limited to lagoons and boat channels which limit spatial sampling and bias measurements against the presence of reef flat plates. Consequently, a static profile approach was chosen, where electrodes were laid by wading in the reef then moved along the direction of the electrode, creating a long pseudo profile.

In this study, an ER system with a specially designed marine cable was deployed (AGI, Austin, Texas, USA). The marine cable is constructed with 28 graphite electrodes spaced 1.5 m apart and waterproofed for marine environments. It was decided to place the electrode cable on the reef floor rather than float it on the water surface to increase subsurface resolution. At one location reported here, a "slide along" survey was conducted by repeating the profile after moving it longitudinally with a 50% overlap of electrode positions. Porewater salinity was derived from inverted electrical resistivity profiles using Archie's Law (Eq. 6) following the approach by Befus et al. (2014).

Numerical modeling of SGD

Hydrogeologic parameters are not sufficiently constrained to conduct calibrated modeling of groundwater transport beneath the reef plate. Simple two-dimensional (2D) profile simulations were developed, however, to examine how relatively buoyant fresh groundwater might behave when confined by a reef flat plate. The generic multi-physics simulator COMSOL was used for this purpose. The simulator accounts for Darcy flow of water driven by pressure and buoyancy forces. Hydraulic conductivities and groundwater specific discharge were based upon those estimated by Oberdorfer and Buddemeier (1986) using borehole dilution tests in the reef flats of the Davies Reef, part of the Great Barrier Reef of Australia. The reef plate was assumed to have a hydraulic conductivity of two orders-of-magnitude less than the underlying reef sediments. Groundwater was released from below the reef plate simulating the observation that the reef plate persists at least 100 m inland, as has been observed in soil excavations by residents on Mo'orea. The ocean water column was modeled as a highly permeable porous medium to allow simulation of standing water in Darcy flow calculations. The top, bottom, and right-side boundary at the reef flat plate and above were designated no flow boundaries (Fig. 8). The right boundary below the reef plate and the left boundary were designated as specified flux. The inlet flux was 0.86 cm/day and outlet flow 1.3 cm/day to preserve mass balance. A transient simulation was conducted, but the flow system rapidly converged to steady conditions.

Even though the adopted modeling parameters for this exercise were derived from comparable reef settings (i.e., Oberdorfer and Buddemeier 1986), the results are by no means considered predictive of specific groundwater flows beneath the Mo'orea fringing reef. Similar to the theoretical study by Houben et al. (2018), the aim is to understand the underlying physics of the submarine confined groundwater flow beneath reefs. In this case, however, the influence of the thin confining reef plate and how breaches in that plate might lead to groundwater fluxes to the coral reef at the seafloor were considered.

Results and discussion

Radon, salinity and tidal stage relationships

Radon values at the three test sites were low, generally ranging from <1,000 to 5,000 dpm/m^3 for both spatial and temporal surveys (Figs. 4 and 5; Table 2). Values of <1,000 dpm/m^3 are typical for ocean surface water and values of <5000 dpm/m^3 could be ambient radon derived from tidal recirculation (Cyronak et al. 2014; Tait et al. 2013).

Tidal amplitudes on Mo'orea are also low (<0.3 m; Knee et al. 2016) and this may explain the somewhat attenuated temporal variability of radon values, with fairly low standard deviations (<1,000 dpm/m^3; Fig. 4) as compared to other volcanic islands with more pronounced tidal ranges (cf. Bishop et al. 2017; Cyronak et al. 2014; Kelly et al. 2019). However, the time series data do not reveal the typical inverse relationship between radon and salinity or tidal stage data (Fig. 4) that

Table 2 Mean total and fresh SGD fluxes calculated from time series and spatial survey data

Study Site	Mean ^{222}Rn Time Series (dpm/m^3)[a]	Mean ^{222}Rn Spatial Survey (dpm/m^3)[a]	Mean Salinity Spatial Survey (ppt)[a]	Mean Depth Spatial Survey (m)[a]	F_{mix} (dpm/m^2/d)[b]	F_{atm} (dpm/m^2/d)[b]	F_{prod} (dpm/m^2/d)[b]	F_{dec} (dpm/m^2/d)[b]	F_{SGD} (dpm/m^2/d)[b]	F_{SGD} (m/d)[b]	F_{SGD} (m^3/m/d)[b]	Fresh F_{SGD} (m^3/m/d)[b]
Northeastern	2508 ± 945	268 ± 350	33.7 ± 1.08	2.42 ± 0.95	641 ± 12.5	7.42 ± 1.32	32.0	108	743 ± 13.8	64.1 ± 1.19 x 10^{-4}	9.63 ± 0.18	0.48 ± 0.01
Western	NC	7729 ± 5736	33.3 ± 0.36	1.15 ± 0.61	7109 ± 138	28,463 ± 2061	15.1	1200	36,756 ± 2199	0.317 ± 0.02	756 ± 45.2	68.4 ± 4.09
Gump Station	1651 ± 871	NC	NC	NC	1371 ± 26.7	28.0 ± 6.07	7.27	182	1280 ± 14.9	110 ± 1.28×10^{-4}	NC	NC

NC = Not Calculated

[a] ± range reflects one standard deviation of measurement range

[b] ± range reflects propagated error from range of estimated water residence time (τ)

would be expected if tidal processes dominate and if SGD is composed of brackish to freshwater. There is also no statistical correlation (Pearson $R < 0.1$; $p > 0.1$) between radon and measured salinity data from the spatial surveys. Collectively, these observations rule out fresh groundwater as a dominant SGD source. The recorded radon pattern is rather more indicative for longshore coastal currents, and, to a lesser degree, tidal mixing. The only high fresh SGD exceptions were a few measurement locations just north of the Western transect where radon levels as high as 21 × 10^3 dpm/m^3 (Fig. 5b) and salinity levels as low as 31.5 were recorded. These records occurred north of the outlet of a non-perennial stream channel that was not flowing (i.e., dried up stream bed) at the time of the study (Fig. 5b). However, there was flowing water at a natural spring located along the streambed about 300 m inland from the shoreline (Fig. 5b). The groundwater end-member for the SGD calculation was established from this spring site. As this spring feeds in to the streambed and as the stream reportedly discharges into the ocean during several months of the year, it was conjectured that episodic streamflow has incised the reef flat plate. Although it was not possible to separate the influence of spring water discharge to the surface water column and spring water that underflows the stream based on the spatial radon surveys, it appears that stream underflow presents a significant source of freshwater to the reef at the Western site.

Discrepancy between radon and water budget-based SGD

The mean radon and salinity data-based estimates of fresh SGD for the Northeastern and Western transects (0.48 and 68.4 m^3/m/day, respectively; Table 2) are lower than the water budget-based SGD values (59.3 and 84.4 m^3/m/day, respectively; Table 1). The difference is particularly striking for the Northeastern transect where the water budget-derived SGD estimate exceeds that from the radon data by a factor >100. If the groundwater radon end-member was raised to a higher value of ~200 × 10^3 dpm/m^3, as was done in SGD analyses on similar volcanic islands (e.g., Bishop et al. 2017; Cyronak et al. 2014), the discrepancy between the water-budget- and radon-derived SGD estimates at the Northeastern site would increase even further, to a factor >200.

These findings are surprising since for a tropical humid setting like Mo'orea, where recharge rates are high, elevated radon (i.e., >5,000 dpm/m^3) would be expected in nearshore surveys if diffuse SGD from the shoreface dominates. Evidence was found for this only along the Western transect where the confining reef plate may have been incised by a non-perennial stream. For the other sites, the data suggest that fresh SGD may not be captured in coastal surveys as it may actually underflow the reef due to the flat plate. There is,

however, uncertainty in the SGD quantification approaches that need to be addressed for further clarification.

Uncertainty in the radon and salinity data-based fresh SGD estimation stems primarily from the inability to reliably (1) establish the groundwater radon and salinity end-members, (2) quantify atmospheric radon losses and (3) estimate mixing with offshore water. More site-specific data on beach pore-water chemistry and coastal water residence times through, e.g., radium ARs and back-reef current measurements, are needed for refined constraints. Furthermore, the inaccurate consideration of detection-equipment response delay complicates a location assessment of fresh SGD hot spots. Similarly, the precision of CTD instrumentation may not be sufficient to resolve fresh SGD components in settings where SGD from tidally recirculated saline SGD dominates. In those instances, it may also be difficult to appropriately account for the depth of the "mixed salinity" layer, which is however critical in the calculation of F_{SGD}. As outlined by Burnett et al. (2006) and Schubert et al. (2014), the best solution may be the use of a combination of tracers, including, e.g., δD and $\delta^{18}O$ isotopes or dissolved Si (e.g., Oehler et al. 2019b) to avoid these pitfalls.

The main limitation of the water budget approach, as applied herein, lies in the inability to account for recharge from cloud water interception or precipitation loss from surface runoff which can be significant on high-level volcanic islands (Giambelluca et al. 2011; Juvik et al. 2011; Juvik and Nullet 1995). Additionally, the low spatial (~1-km^2 grid size) and temporal (monthly frequency) resolution of P and ET input data really hamper a reliable assessment of watershed-scale specific parameters. More data from spatially distributed meteorological stations and streamflow gages would certainly lead to improved estimates of recharge and maximum fresh SGD.

Despite these uncertainties, analyses from this study indicate that shoreline SGD fluxes to the reef are generally insignificant compared with marine currents. This is especially true of measurements made at Gump Station and the Northeastern site which were generally close (i.e., less than 100 m) to the shore. Exceptions to these observations are outlets of perennial streams (e.g., Cook's Bay and Opunohu Bay) as noted by Knee et al. (2016), or small spring-fed streams as sampled near the Western study site, where radon and reduced salinity were detected as far offshore as 300 m (Fig. 5b). Lava tubes may discharge freshwater offshore, as is observed in many other young volcanic islands (e.g., Bishop et al. 2017; Dimova et al. 2012; Tait et al. 2013), but it was not possible to confirm the occurrence of these in the field. Furthermore, the northeastern corner of the island is dominated by a carbonate shelf which, based on studies from similar environments, may also have the potential to discharge groundwater through karstic subsurface features (e.g., Cardenas et al. 2010; Null et al. 2014). Further research in these areas of the island is recommended for clarification.

Electrical resistivity profiles

The inverted ER profiles are shown in terms of electrical conductivity (the inverse of electrical resistivity) in units of mS/m in Fig. 7. The seawater has an electrical conductivity of about 5,000 mS/m. Based upon field observations, the shallow depth of the ER profiles and the age of the last volcanic activity on the island (>500 ka; Hildenbrand et al. 2005), there is confidence that volcanic flows do not extend from the shoreline, and that the reef material is entirely carbonate. However, the porosity and pore connectivity (n and m in Eq. 6) are not known. Oberdorfer and Buddemeier (1986) drilled boreholes into shallow reefs off the coast of NE Australia and found that sediments were occasionally karstic beneath the reef flat plate, but could also be composed of unconsolidated carbonate sediments. Karst-like features have been documented in numerous Pleistocene-aged limestones below reefs, apparently formed during periods of low-sea level stands (Woodroffe 2008).

Lacking other information, the relationship between bulk resistivity and fluid resistivity was followed as described by Cardenas et al. (2010) and Befus et al. (2014), noting that their surveys imaged also lava flows. According to their studies, very porous carbonate sediments saturated with seawater has an electrical conductivity of about 2,000 mS/m (i.e. $n = 0.6$ and $m = 2$). The color scale applied in Fig. 7, therefore, shows seawater in red (5000 mS/m), seawater-saturated carbonates in yellow (~2,000 mS/m), and freshened pore water in green and blue (<2,000 mS/m).

Figure 7 suggests that there is freshened water within the reef structure. The section at Gump Station (Fig. 7a) shows a decrease in electrical conductivity (EC) below the seafloor along the nearly entire 26 m survey. At the elevation drop in the reef (0-5 m of survey coordinates), EC increases, likely because of an increase in porosity due to a thickening of loose coral detritus. The Western section (Fig. 7b) shows similar freshening below the reef but only closer to shore (10–26.5 m in survey coordinates). If the increase in conductivity is due to groundwater flow to the reef, then it is not obvious why the freshened water does not extend further out. It may discharge to the water column, but radon measurements did not detect such seepage, possibly due to seawater dilution in the deep water column. It is also possible that the water moves laterally along the reef, parallel to shore. About 100 m to the south of this section, the reef is incised by an ephemeral stream (as supported through radon surveys) that may serve as a discharge feature for groundwater. The Northeastern section, which was produced using a slide-along merging of multiple 26-m surveys (50% overlap), shows the lowest EC of the three sections. EC is mostly below 1,500 mS/m with a zone of slightly lower EC at about 3 m depth and a localized zone of very low EC of less than 500 mS/m in the middle of the survey (40-60 m survey coordinate). This EC is an order of

magnitude below seawater EC and is good evidence of freshened water.

Overall, the surveys suggest freshened water exists very close to the marine water column, consistent with a thin (<1 m) reef flat plate confining groundwater. Using reasonable parameters for Archie's Law (Eq. 6) for the Western and Gump Station sites, one could arrive at the similar reductions in EC through increases in porosity. This is particularly true if the pore-connectivity parameter (m) is larger than 2, which has been suggested for vuggy carbonates (Jackson et al. 2002, 1993). The EC of 500 mS/m in the Northeastern section is difficult to explain by porosity increases in the absence of karstic voids. As there are no obvious indications of well-developed karst, e.g., collapse features or sink holes, the evidence suggests the low EC values measured at this section indicate freshened water confined below the reef flat plate.

Numerical modeling

To evaluate the efficacy of groundwater underflow in the reef, a series of numerical simulations were performed that account for fluid density contrasts as explained in section 'Numerical modeling of SGD'. Freshwater was released below the reef plate and rose buoyantly as it migrated away from the shoreline. Salinity is normalized between fresh (0 or blue) and seawater (1 or red) in the color mapped cross sections (Fig. 8). The color scale applied in Fig. 8 is similar to that in Fig. 7 with seawater in red, seawater-saturated carbonates in yellow, and freshened pore water in green and blue. Figure 8 compares two scenarios of groundwater flow beneath the reef flat plate. In the first scenario, the reef flat plate, outlined in black, is completely confining and continuous, and in the second scenario the reef flat plate is breached, say, by a fissure. In both scenarios, the reef flat plate is assumed to increase in depth as it approaches the edge of the reef, similar to the scenario shown Fig. 7.

When the reef plate is continuous (Fig. 8a), the relatively buoyant freshwater is entirely confined by the reef flat plate. Breaches in the plate (Fig. 8b), however, can cause submarine seeps to develop that may impact the reef environment. Seeps are more significant closer to shore where confined head is largest. While conducting the field surveys, there was at least one location where noticeably colder water was seeping up through the reef bed. The next day, however, when prevailing winds drove more water into the lagoon, the spring no longer flowed, even at low tide.

Conclusions and implications

Water budget analysis, radon surveying and geophysical imaging suggest the presence of freshened groundwater below the fringing reef off Mo'orea. The preliminary interpretation is that SGD occurs by groundwater discharging at the coast primarily below the reef flat plate, which extends on shore, roughly coincident with the water table. This conclusion is based upon the suggestion of freshened water below the reef flat plate by ER surveys, and the evidential lack of terrestrial groundwater in the water column above the reef, as indicated by the discrepancy between water budget-based and radon surveying based fresh SGD estimates (Tables 1 and 2). These results, based only upon three selected transect sites, do not unequivocally demonstrate either the ubiquitous presence of freshwater below the reef or a lack of coastal groundwater discharge to the reef in general. However, they do suggest that the reef flat plate identified in other tropical reefs, principally atolls, may have an important influence on SGD fluxes to reefs on volcanic islands as well. Reef flat plates are highly lithified and apparently of relatively low permeability so it may be an effective confining unit that traps groundwater flow below the reef. It is not clear where groundwater ultimately discharges if it is constrained beneath the reef flat plate. The ER transects and numerical models suggest that freshened groundwater may travel both parallel and perpendicular to the shoreline, so fresh groundwater may flow to the reef plate perimeter at the reef crest or to local discharge locations such as those created through incision by ephemeral streams. Other researchers have found that sediments below the reef flat plate may be semilithified and/or karstic, further complicating the behavior of reef hydrogeology (Ayers and Vacher 1986).

Review of the literature concerning SGD to tropical reefs indicates a strong bias toward sampling of known sources of groundwater discharge, e.g., from stream underflow, lava tubes, or fissures/craters in volcanic lithologies. Understanding the spatial distribution of groundwater movement to and through the reef is an important precursor to upscaling point samples to total flux estimates of SGD to reefs. To date, most estimates of SGD fluxes to tropical reefs have assumed that point measurements of SGD are representative of SGD fluxes as a whole. In addition, estimates for coral reef settings have assumed that SGD occurs primarily at the shoreline (e.g., Paytan et al. 2006). This study, and other ER studies of reefs, suggest that discrete geologic features such as faults, fractures, lava tubes, or karst may generate highly heterogeneous and off-shore SGD. Consequently, further studies of subreef hydrogeology are warranted, particularly if they result in upscaled estimates of geochemical fluxes of SGD.

Acknowledgements We are indebted to Megan Donahue, Henry Shui, and Danielle Barnas for their help and support with fieldwork and to Doug Hammond for the analysis of ^{226}Ra activities at USC. We also thank Neil Davies, Teurumereariki Hinano Murphy, Valentine Brotherson and Jacques You Sing from Gump Station for logistic support. We are furthermore grateful for the constructive comments of two anonymous reviewers. This study was funded by U.S. National Science

Foundation HS-1936671 to BH and MB and OCE-1924281 to NJS (CSUN Marine Biology contribution No. 305). Some resources were provided by the Mo'orea Coral Reef LTER, which is supported by the U.S. National Science Foundation under Grant (OCE#16-37396) as well as a generous gift from the Gordon and Betty Moore Foundation.

References

Amato DW, Bishop JM, Glenn CR, Dulai H, Smith CM (2016) Impact of submarine groundwater discharge on marine water quality and reef biota of Maui. PLOS ONE 11:e0165825. https://doi.org/10.1371/journal.pone.0165825

Anthony SS (2004) Hydrogeology of selected islands of the Federated States of Micronesia, chap 24. In: Geology and hydrogeology of carbonate islands. Developments in Sedimentology 54, Elsevier, Amsterdam, pp 693–706

Ayers JF, Vacher HL (1986) Hydrogeology of an atoll island: a conceptual model from detailed study of a Micronesian example. Groundwater 24:185–198. https://doi.org/10.1111/j.1745-6584.1986.tb00994.x

Bailey R, Jenson J, Rubinstein D, Olsen A (2008) Groundwater resources of atoll islands: observations, modelling and management: technical report 119. Water and Environmental Research Institute of the Western Pacific, University of Guam, Mangilao, Guam

Bailey RT, Jenson JW, Olsen AE (2009) Numerical modeling of atoll island hydrogeology. Ground Water 47:184–196

Bailey RT, Jenson JW, Olsen AE (2010) Estimating the ground water resources of atoll islands. Water 2(1):1–27

Barillon R, Özgümüs A, Chambaudet A (2005) Direct recoil radon emanation from crystalline phases: influence of moisture content. Geochim Cosmochim Acta 69:2735–2744. https://doi.org/10.1016/j.gca.2004.11.021

Befus KM, Cardenas MB, Tait DR, Erler DV (2014) Geoelectrical signals of geologic and hydrologic processes in a fringing reef lagoon setting. J Hydrol 517:508–520. https://doi.org/10.1016/j.jhydrol.2014.05.070

Bishop JM, Glenn CR, Amato DW, Dulai H (2017) Effect of land use and groundwater flow path on submarine groundwater discharge nutrient flux. J Hydrol Reg Stud 11:194–218. https://doi.org/10.1016/j.ejrh.2015.10.008

Bojanowski R (1988) Inventory of radium isotopes in the oceans. No. IAEA-TECDOC-481, IAEA, Geneva

Burnett WC, Dulaiova H (2003) Estimating the dynamics of groundwater input into the coastal zone via continuous radon-222 measurements. J Environ Radioact 2001:21–35. https://doi.org/10.1016/S0265-931X(03)00084-5

Burnett WC, Aggarwal PK, Aureli A, Bokuniewicz H, Cable JE, Charette MA, Kontar E, Krupa S, Kulkarni KM, Loveless A, Moore WS, Oberdorfer JA, Oliveira J, Ozyurt N, Povinec P, Privitera AMG, Rajar R, Ramessur RT, Scholten J, Stieglitz T, Taniguchi M, Turner JV (2006) Quantifying submarine groundwater discharge in the coastal zone via multiple methods. Sci Total Environ 367:498–543. https://doi.org/10.1016/j.scitotenv.2006.05.009

Cardenas MB, Zamora PB, Siringan FP, Lapus MR, Rodolfo RS et al (2010) Linking regional sources and pathways for submarine groundwater discharge at a reef by electrical resistivity tomography, 222Rn, and salinity measurements. Geophys Res Lett 37. https://doi.org/10.1029/2010GL044066

Cecil LD, Green JR (2000) Radon-222. In: Cook PG, Herczeg AL (eds) Environmental tracers in subsurface hydrology. Springer, Boston, pp 175–194. https://doi.org/10.1007/978-1-4615-4557-6_6

Comeau S, Edmunds PJ, Lantz CA, Carpenter RC (2014) Water flow modulates the response of coral reef communities to ocean acidification. Sci Rep 4:1–6. https://doi.org/10.1038/srep06681

Cook PG, Favreau G, Dighton JC, Tickell S (2003) Determining natural groundwater influx to a tropical river using radon, chlorofluorocarbons and ionic environmental tracers. J Hydrol 277:74–88

Crook ED, Potts D, Rebolledo-Vieyra M, Hernandez L, Paytan A (2012) Calcifying coral abundance near low-pH springs: implications for future ocean acidification. Coral Reefs 31:239–245. https://doi.org/10.1007/s00338-011-0839-y

Cuet P, Atkinson MJ, Blanchot J, Casareto BE, Cordier E, Falter J, Frouin P, Fujimura H, Pierret C, Susuki Y, Tourrand C (2011) CNP budgets of a coral-dominated fringing reef at La Réunion, France: coupling of oceanic phosphate and groundwater nitrate. Coral Reefs 30:45. https://doi.org/10.1007/s00338-011-0744-4

Cyronak T, Santos IR, Erler DV, Eyre BD (2013) Groundwater and porewater as major sources of alkalinity to a fringing coral reef lagoon (Muri Lagoon, Cook Islands). Biogeosciences 10:2467–2480. https://doi.org/10.5194/bg-10-2467-2013

Cyronak T, Santos IR, Erler DV, Maher DT, Eyre BD (2014) Drivers of pCO2 variability in two contrasting coral reef lagoons: the influence of submarine groundwater discharge. Glob Biogeochem Cycles 28:398–414. https://doi.org/10.1002/2013GB004598

Dickinson WR (2004) Impacts of eustasy and hydro-eustasy on the evolution and landforms of Pacific atolls. Palaeogeogr Palaeoclimatol Palaeoecol 213:251–269

Dimova NT, Swarzenski PW, Dulaiova H, Glenn CR (2012) Utilizing multichannel electrical resistivity methods to examine the dynamics of the fresh water–seawater interface in two Hawaiian groundwater systems. J Geophys Res Oceans 117. https://doi.org/10.1029/2011JC007509

Dubé CE, Mercière A, Vermeij MJA, Planes S (2017) Population structure of the hydrocoral *Millepora platyphylla* in habitats experiencing different flow regimes in Moorea, French Polynesia. PLOS ONE 12:e0173513. https://doi.org/10.1371/journal.pone.0173513

Edmunds P, Adam T, Baker A, Doo S, Glynn P, Manzello D, Silbiger N, Smith T, Fong P (2018) Why more comparative approaches are required in time-series analyses of coral reef ecosystems. Mar Ecol Prog Ser 608:297–306. https://doi.org/10.3354/meps12805

Engott JA, Johnson AG, Bassiouni M, Izuka SK, Rotzoll K (2017) Spatially distributed groundwater recharge for 2010 land cover estimated using a water-budget model for the Island of O'ahu, Hawai'i. US Geol Surv Sci Invest Rep 2015-5010

Eyre BD, Andersson AJ, Cyronak T (2014) Benthic coral reef calcium carbonate dissolution in an acidifying ocean. Nat Clim Change 4:969–976. https://doi.org/10.1038/nclimate2380

Eyre BD, Cyronak T, Drupp P, Carlo EHD, Sachs JP, Andersson AJ (2018) Coral reefs will transition to net dissolving before end of century. Science 359:908–911. https://doi.org/10.1126/science.aao1118

Falkland AC (1994) Climate, Hydrology and water resources of the Cocos (Keeling) Islands. Atoll Res Bull 400:1–23

Fick SE, Hijmans RJ (2017) WorldClim 2: new 1-km spatial resolution climate surfaces for global land areas. Int J Climatol 37:4302–4315. https://doi.org/10.1002/joc.5086

Garrison GH, Glenn CR, McMurtry GM (2003) Measurement of submarine groundwater discharge in Kahana Bay, O'ahu, Hawai'i. Limnol Oceanogr 48:920–928. https://doi.org/10.4319/lo.2003.48.2.0920

Giambelluca TW, DeLay JK, Nullet MA, Scholl MA, Gingerich SB (2011) Canopy water balance of windward and leeward Hawaiian cloud forests on Haleakalā, Maui, Hawai'i. Hydrol Process 25:438–447

Gingerich SB, Voss CI (2005) Three-dimensional variable-density flow simulation of a coastal aquifer in southern Oahu, USA. Hydrogeol J 13:436–450

Gove JM, McManus MA, Neuheimer AB, Polovina JJ, Drazen JC, Smith CR, Merrifield MA, Friedlander AM, Ehses JS, Young CW, Dillon AK, Williams GJ (2016) Near-island biological hotspots in barren

ocean basins. Nat Commun 7:10581. https://doi.org/10.1038/ncomms10581

Grossman EE, Barnhardt WA, Hart P, Richmond BM, Field ME (2006) Shelf stratigraphy and the influence of antecedent substrate on Holocene reef development, south Oahu, Hawaii. Mar Geol 226: 97–114. https://doi.org/10.1016/j.margeo.2005.09.012

Hagedorn B, El-Kadi A, Mair A, Whittier R, Ha K (2011) Estimating recharge in fractured aquifers of a temperate humid to semiarid volcanic island (Jeju, Korea) from water table fluctuations, and Cl, CFC-12 and 3H chemistry. J Hydrol 409:650–662. https://doi.org/10.1016/j.jhydrol.2011.08.060

Hagedorn B, El-Kadi A, Whittier R (2016) Controls on the δ13CDIC and alkalinity budget of a flashy subtropical stream (Manoa River, Hawaii). Appl Geochem 73. https://doi.org/10.1016/j.apgeochem.2016.07.008

Harlow J, Hagedorn B (2019) SWB modeling of groundwater recharge on Catalina Island, California, during a period of severe drought. Water 11:58. https://doi.org/10.3390/w11010058

Haßler K, Dähnke K, Kölling M, Sichoix L, Nickl A-L, Moosdorf N (2019) Provenance of nutrients in submarine fresh groundwater discharge on Tahiti and Moorea, French Polynesia. Appl Geochem 100:181–189. https://doi.org/10.1016/j.apgeochem.2018.11.020

Hemmings B, Whitaker F, Gottsmann J, Hughes A (2015) Hydrogeology of Montserrat review and new insights. J Hydrol Reg Stud 3:1–30. https://doi.org/10.1016/j.ejrh.2014.08.008

Hench JL, Leichter JJ, Monismith SG (2008) Episodic circulation and exchange in a wave-driven coral reef and lagoon system. Limnol Oceanogr 53:2681–2694. https://doi.org/10.4319/lo.2008.53.6.2681

Hijmans RJ, Cameron SE, Parra JL, Jones PG, Jarvis A (2005) Very high resolution interpolated climate surfaces for global land areas. Int J Climatol 25:1965–1978. https://doi.org/10.1002/joc.1276

Hildenbrand A, Marlin C, Conroy A, Gillot P-Y, Filly A, Massault M (2005) Isotopic approach of rainfall and groundwater circulation in the volcanic structure of Tahiti-Nui (French Polynesia). J Hydrol 302:187–208. https://doi.org/10.1016/j.jhydrol.2004.07.006

Houben GJ, Stoeckl L, Mariner KE, Choudhury AS (2018) The influence of heterogeneity on coastal groundwater flow: physical and numerical modeling of fringing reefs, dykes and structured conductivity fields. Adv Water Resour 113:155–166. https://doi.org/10.1016/j.advwatres.2017.11.024

Izuka SK, Oki DS, Chen C (2005) Effects of irrigation and rainfall reduction on ground-water recharge in the Lihue Basin, Kauai, Hawaii. US Geol Surv Sci Invest Rep 2005-5146, 48 pp

Jackson PD, Jarrard RD, Pigram CJ, Pearce JM (1993) Resistivity/porosity/velocity relationships from downhole logs: an aid for evaluating pore morphology, chap 45. In: Proceedings of the Ocean Drilling Program, Scientific Results 142, Texas A&M, College Station, TX

Jackson PD, Briggs KB, Flint RC, Holyer RJ, Sandidge JC (2002) Two- and three-dimensional heterogeneity in carbonate sediments using resistivity imaging. Mar Geol 182:55–76. https://doi.org/10.1016/S0025-3227(01)00228-6

Johnson AG, Engott JA, Bassiouni M, Rotzoll K (2018) Spatially distributed groundwater recharge estimated using a water-budget model for the Island of Maui, Hawai`i, 1978–2007. US Geol Surv Sci Invest Rep 2014-5168

Juvik JO, Nullet D (1995) Relationships between rainfall, cloud-water interception and canopy throughfall in a Hawaiian montane forest. In: Hamilton LS, Juvik JO, Scatena FN (eds) Tropical montane cloud forests. Springer, New York, pp 165–182

Juvik JO, DeLay JK, Kinney KM, Hansen EW (2011) A 50th anniversary reassessment of the seminal 'Lāna'i fog drip study' in Hawai'i. Hydrol Process 25:402–410

Kelly JL, Dulai H, Glenn CR, Lucey PG (2019) Integration of aerial infrared thermography and in situ radon-222 to investigate submarine groundwater discharge to Pearl Harbor, Hawaii, USA. Limnol Oceanogr 64:238–257. https://doi.org/10.1002/lno.11033

Knee KL, Street JH, Grossman EE, Boehm AB, Paytan A (2010) Nutrient inputs to the coastal ocean from submarine groundwater discharge in a groundwater-dominated system: relation to land use (Kona coast, Hawaii, U.S.A.). Limnol Oceanogr 55:1105–1122. https://doi.org/10.4319/lo.2010.55.3.1105

Knee KL, Crook ED, Hench JL, Leichter JJ, Paytan A (2016) Assessment of submarine groundwater discharge (SGD) as a source of dissolved radium and nutrients to Moorea (French Polynesia) coastal waters. Estuaries Coasts 39:1651–1668. https://doi.org/10.1007/s12237-016-0108-y

Koh G-W, Kang B-R, Moon D-C (2006) Hydro-geological features and groundwater management systems of Jeju Island. Proc Jeju Hawaii Water Forum, Jeju, Korea, July 2006, pp 325–362

Lau LS, Mink JF (2006) Hydrology of the Hawaiian Islands. University of Hawai'i Press, Honolulu

Leichter JJ, Aildredge AL, Bernardi G, Brooks A, Carlson C, Carpenter RC, Edmunds P, Fewing MR, Hanson K, Hench JL, Holbrook SJ, Nelson C, Toonen R, Washburn L, Wyatt A (2013) Biological and physical interactions on a tropical island coral reef: transport and retention processes around Moorea, French Polynesia. Oceanography 26:52–63

Lubarsky KA, Silbiger NJ, Donahue MJ (2018) Effects of submarine groundwater discharge on coral accretion and bioerosion on two shallow reef flats. Limnol Oceanogr 63:1660–1676. https://doi.org/10.1002/lno.10799

Macintyre IG (1977) Distribution of submarine cements in a modern Caribbean fringing reef, Galeta Point, Panama. J Sediment Res 47: 503–516. https://doi.org/10.1306/212F71C1-2B24-11D7-8648000102C1865D

Macintyre IG (2011) Submarine lithification. In: Hopley D (ed) Encyclopedia of modern coral reefs: structure, form and process. Springer, Dordrecht, The Netherlands, pp 1052–1058. https://doi.org/10.1007/978-90-481-2639-2_28

Mair A, Johnson AG, Rotzoll K, Oki DS (2019) Estimated groundwater recharge from a water-budget model incorporating selected climate projections, Island of Maui, Hawai'i. US Geol Surv Sci Invest Rep 2019-5064

McMahon A, Santos IR (2017) Nitrogen enrichment and speciation in a coral reef lagoon driven by groundwater inputs of bird guano. J Geophys Res Oceans 122:7218–7236

Montiel D, Dimova N, Andreo B, Prieto J, García-Orellana J, Rodellas V (2018) Assessing submarine groundwater discharge (SGD) and nitrate fluxes in highly heterogeneous coastal karst aquifers: challenges and solutions. J Hydrol 557:222–242. https://doi.org/10.1016/j.jhydrol.2017.12.036

Mu Q, Heinsch FA, Zhao M, Running SW (2007) Development of a global evapotranspiration algorithm based on MODIS and global meteorology data. Remote Sens Environ 111:519–536. https://doi.org/10.1016/j.rse.2007.04.015

Mu Q, Zhao M, Running SW (2011) Improvements to a MODIS global terrestrial evapotranspiration algorithm. Remote Sens Environ 115: 1781–1800. https://doi.org/10.1016/j.rse.2011.02.019

Nelson CE, Donahue MJ, Dulaiova H, Goldberg SJ, La Valle FF, Lubarsky K, Miyano J, Richardson C, Silbiger NJ, Thomas FIM (2015) Fluorescent dissolved organic matter as a multivariate biogeochemical tracer of submarine groundwater discharge in coral reef ecosystems. Mar Chem 177:232–243. https://doi.org/10.1016/j.marchem.2015.06.026

Null KA, Knee KL, Crook ED, de Sieyes NR, Rebolledo-Vieyra M, Hernández-Terrones L, Paytan A (2014) Composition and fluxes of submarine groundwater along the Caribbean coast of the Yucatan Peninsula. Cont Shelf Res 77:38–50. https://doi.org/10.1016/j.csr.2014.01.011

Oberdorfer JA, Buddemeier RW (1986) Coral-reef hydrology: field studies of water movement within a barrier reef. Coral Reefs 5:7–12. https://doi.org/10.1007/BF00302165

Oehler T, Bakti H, Lubis RF, Purwoarminta A, Delinom R, Moosdorf N (2019a) Nutrient dynamics in submarine groundwater discharge through a coral reef (western Lombok, Indonesia). Limnol Oceanogr 64:2646–2661. https://doi.org/10.1002/lno.11240

Oehler T, Tamborski J, Rahman S, Moosdorf N, Ahrens J, Mori C, Neuholz R, Schnetger B, Beck M (2019b) DSi as a tracer for submarine groundwater discharge. Front Mar Sci 6. https://doi.org/10.3389/fmars.2019.00563

Oki DS, Souza WR, Bolke EL, Bauer GR (1998) Numerical analysis of the hydrogeologic controls in a layered coastal aquifer system, Oahu, Hawaii, USA. Hydrogeol J 6:243–263. https://doi.org/10.1007/s100400050149

Paerl HW (1997) Coastal eutrophication and harmful algal blooms: importance of atmospheric deposition and groundwater as "new" nitrogen and other nutrient sources. Limnol Oceanogr 42:1154–1165. https://doi.org/10.4319/lo.1997.42.5_part_2.1154

Parnell K (1986) Water movement within a fringing reef flat, Orpheus Island, North Queensland, Australia. J Int Soc Reef Stud 5:1–6. https://doi.org/10.1007/BF00302164

Parra SM, Valle-Levinson A, Mariño-Tapia I, Enriquez C (2015) Salt intrusion at a submarine spring in a fringing reef lagoon. J Geophys Res Oceans 120:2736–2750. https://doi.org/10.1002/2014JC010459

Paytan A, Shellenbarger GG, Street JH, Gonneea ME, Davis K, Young MB, Moore WS (2006) Submarine groundwater discharge: an important source of new inorganic nitrogen to coral reef ecosystems. Limnol Oceanogr 51:343–348. https://doi.org/10.4319/lo.2006.51.1.0343

Petermann E, Schubert M (2015) Quantification of the response delay of mobile radon-in-air detectors applied for detecting short-term fluctuations of radon-in-water concentrations. Eur Phys J Spec Top 224:697–707. https://doi.org/10.1140/epjst/e2015-02400-5

Peterson RN, Burnett WC, Glenn CR, Johnson AG (2009) Quantification of point-source groundwater discharges to the ocean from the shoreline of the Big Island, Hawaii. Limnol Oceanogr 54:890–904. https://doi.org/10.4319/lo.2009.54.3.0890

Povinec PP, Burnett WC, Beck A, Bokuniewicz H, Charette M, Gonneea ME, Groening M, Ishitobi T, Kontar E, Liong Wee Kwong L, Marie DEP, Moore WS, Oberdorfer JA, Peterson R, Ramessur R, Rapaglia J, Stieglitz T, Top Z (2012) Isotopic, geophysical and biogeochemical investigation of submarine groundwater discharge: IAEA-UNESCO intercomparison exercise at Mauritius Island. J Environ Radioact 104:24–45. https://doi.org/10.1016/j.jenvrad.2011.09.009

Prouty NG, Cohen A, Yates KK, Storlazzi CD, Swarzenski PW, White D (2017) Vulnerability of coral reefs to bioerosion from land-based sources of pollution. J Geophys Res Oceans 122:9319–9331. https://doi.org/10.1002/2017JC013264

Rad SD, Allègre CJ, Louvat P (2007) Hidden erosion on volcanic islands. Earth Planet Sci Lett 262:109–124. https://doi.org/10.1016/j.epsl.2007.07.019

Richardson CM, Dulai H, Popp BN, Ruttenberg K, Fackrell JK (2017) Submarine groundwater discharge drives biogeochemistry in two Hawaiian reefs. Limnol Oceanogr 62:S348–S363. https://doi.org/10.1002/lno.10654

Rosman JH, Hench JL (2011) A framework for understanding drag parameterizations for coral reefs. J Geophys Res Oceans 116. https://doi.org/10.1029/2010JC006892

Rotzoll K, Oki D, El-Kadi AI (2010) Changes of freshwater-lens thickness in basaltic island aquifers overlain by thick coastal sediments. Hydrogeol J 18:1425–1436

Rougerie F, Fichez R, Dejardin, P (2004) Geomorphology and hydrogeology of selected islands of French Polynesia: Tikehau (Atoll) and Tahiti (Barrier Reef). In: Geology and hydrogeology of carbonate islands. Develop Sedimentol 54:475–502.

Rushton KR, Ward C (1979) The estimation of groundwater recharge. J Hydrol 41:345–361

Santos IR, Erler D, Tait D, Eyre BD (2010) Breathing of a coral cay: Tracing tidally driven seawater recirculation in permeable coral reef sediments. J Geophys Res Oceans 115:10

Sawyer AH, David CH, Famiglietti JS (2016) Continental patterns of submarine groundwater discharge reveal coastal vulnerabilities. Science 353:705–707. https://doi.org/10.1126/science.aag1058

Schubert M, Petermann E, Stollberg R, Gebel M, Scholten J, Knöller K, Lorz C, Glück F, Riemann K, Weiß H (2019) Improved approach for the investigation of submarine groundwater discharge by means of radon mapping and radon mass balancing. Water 11:749. https://doi.org/10.3390/w11040749

Schubert M, Scholten J, Schmidt A, Comanducci JF, Pham MK, Mallast U, Knoeller K (2014) Submarine groundwater discharge at a single spot location: evaluation of different detection approaches. Water 6:584–601

Silbiger NJ, Nelson CE, Remple K, Sevilla JK, Quinlan ZA, Putnam HM, Fox MD, Donahue MJ (2018) Nutrient pollution disrupts key ecosystem functions on coral reefs. https://doi.org/10.5061/dryad.nm1ns61

Street JH, Knee KL, Grossman EE, Paytan A (2008) Submarine groundwater discharge and nutrient addition to the coastal zone and coral reefs of leeward Hawaii. Mar Chem 109:355–376

Tait DR, Santos IR, Erler DV, Befus KM, Cardenas MB, Eyre BD (2013) Estimating submarine groundwater discharge in a South Pacific coral reef lagoon using different radioisotope and geophysical approaches. Mar Chem 156:49–60. https://doi.org/10.1016/j.marchem.2013.03.004

Tait DR, Erler DV, Santos IR, Cyronak TJ, Morgenstern U, Eyre BD (2014) The influence of groundwater inputs and age on nutrient dynamics in a coral reef lagoon. Mar Chem 166:36–47. https://doi.org/10.1016/j.marchem.2014.08.004

Tomlinson MS, De Carlo EH (2003) The need for high resolution time series data to characterize Hawaiian streams. J Am Water Resour Assoc 39:113–123

Tribble GW, Sansone FJ, Buddemeier RW, Li Y-H (1992) Hydraulic exchange between a coral reef and surface sea water. GSA Bull 104:1280–1291. https://doi.org/10.1130/0016-7606(1992)104<1280:HEBACR>2.3.CO;2

Vacher HL (2007) Introduction: Varieties of carbonate islands and a historical perspective. In: Vacher HL, Quinn T (eds) Geology and hydrogeology of carbonate islands. Developments in Sedimentology, vol 54, Elsevier, Amsterdam, pp 1–33

Wang G, Jing W, Wang S, Xu Y, Wang Z, Zhang Z, Li Q, Dai M (2014) Coastal acidification induced by tidal-driven submarine groundwater discharge in a coastal coral reef system. Environ Sci Technol 48:13069–13075. https://doi.org/10.1021/es5026867

Wanninkhof R (2014) Relationship between wind speed and gas exchange over the ocean revisited. Limnol Oceanogr Methods 12:351–362. https://doi.org/10.4319/lom.2014.12.351

Weigel F (1978) Radon. Chem Ztg 102:287–299

Werner AD, Sharp HK, Galvis SC, Post VEA, Sinclair P (2017) Hydrogeology and management of freshwater lenses on atoll islands: Review of current knowledge and research needs. J Hydrol https://doi.org/10.1016/j.jhydrol.2017.02.047

Woodroffe CD (2008) Reef-island topography and the vulnerability of atolls to sea-level rise. Glob Planet Change 62:77–96. https://doi.org/10.1016/j.gloplacha.2007.11.001